Hindawi Publishing Corporation
International Journal of Polymer Science
Volume 2013, Article ID 156289, 10 pages
http://dx.doi.org/10.1155/2013/156289

Research Article

Synthesis and Characterizations of Poly(trimethylene terephthalate)-*b*-poly(tetramethylene glycol) Copolymers

Feng Liu, Meng Yao, and Ming-tao Run

College of Chemistry & Environmental Science, Hebei University, Baoding 071002, China

Correspondence should be addressed to Ming-tao Run; lhbx@hbu.cn

Received 30 June 2013; Revised 1 October 2013; Accepted 1 October 2013

Academic Editor: Giridhar Madras

A series of poly(trimethylene terephthalate)-*b*-poly(tetramethylene glycol) (PTT-PTMEG) copolymers were synthesized by two-step melt-polycondensation. The copolymers were characterized by using Fourier transform infrared spectroscopy (FTIR), ^{1}H NMR spectroscopy, rheometer, differential scanning calorimetry (DSC), polarized optical microscopy (POM), thermal gravimetric analysis (TGA), and mechanical properties. The results suggest that by increasing the flexible PTMEG contents from 0% to 60 wt%, the copolymers show decreased glass transition temperatures, melting points, melt-crystallization temperatures, hardness, tensile strength, thermostability, and smaller spherulites dimensions; however it has much increased impact strength and elongation at breaking point. Compared with commercial poly(butylene terephthalate) (PBT)-type TPEE with 25 mol% flexible segments, PTT-type TPEE having 25 mol% flexible segments has a lower glass transition temperature, melting point, crystallization temperature, and much lower tensile strength although it has a much higher impact strength than that of PBT-type TPEE, and it is not suitably used as a commercial TPEE.

1. Introduction

Thermoplastic polyester elastomers (TPEEs) are linear block copolymers which contain rigid polyester segments and soft polyether segments [1]. In TPEE, both polyether segments and uncrystallized polyester form amorphous phase, while some of the rigid polyester segments form crystals that play the role of physical cross-linking points; thus, TPEEs possess both the elasticity of the rubber and good processability of the thermoplastics. By varying the content of flexible and rigid segments along the chains, the mechanical properties can be adjusted to meet the requirements. Therefore, intensive studies have been carried out on this kind of polymer material. Poly(butylene terephthalate) (PBT) is an industrially used rigid segment in TPEE, and this PBT-type TPEE shows excellent mechanical properties [1]. Polyglycol ether was first introduced to poly(ethylene terephthalate) molecular chains by Du Pont Company, which had better hydrophilicity thus improving the dye ability of products (Hytrel). Multiple TPEE products were developed successively by Toyobo company (Pelprene), GE company (Lomed), Hoechst Celanese company (Retiflex), DSM company (Arnitel), and Elana company (Elitel), and they have been widely used in many fields such as auto manufactory, cable wire, electronic appliances, industrial products, and sports goods [2]. Witsiepe synthesized a poly(ether-ester) by the transesterification and polycondensation in the melt of dimethyl terephthalate and 1,4-butanediol [2]. Nishimura and Kornogata synthesized a kind of poly(ether-ester) elastic fiber based on PBT as rigid segments and poly(tetramethylene glycol) (PTMEG) as polyether flexible segments; this kind of fiber had good tensile elastic recovery at room temperature but relatively poor at 100°C which can be improved by adding a bit monomer of trifunctionality [3]. In order to obtain a new type of TPEE, the rigid segments other than PBT have been changed and applied in the synthesis of new TPEE. In addition to PBT, poly(ethylene terephthalate) (PET) [1, 4], poly(butylene 2,6-naphthalene dicarboxylate) [5, 6], poly(butylene-co-isophthalate) [7], and aromatic polycarbonate [8] were used as rigid segments.

As a linear aromatic polyester, poly(trimethylene terephthalate) (PTT) was first produced by Shell Chemicals Co. (Corterra) [9, 10]. Compared to PBT and PET, PTT has

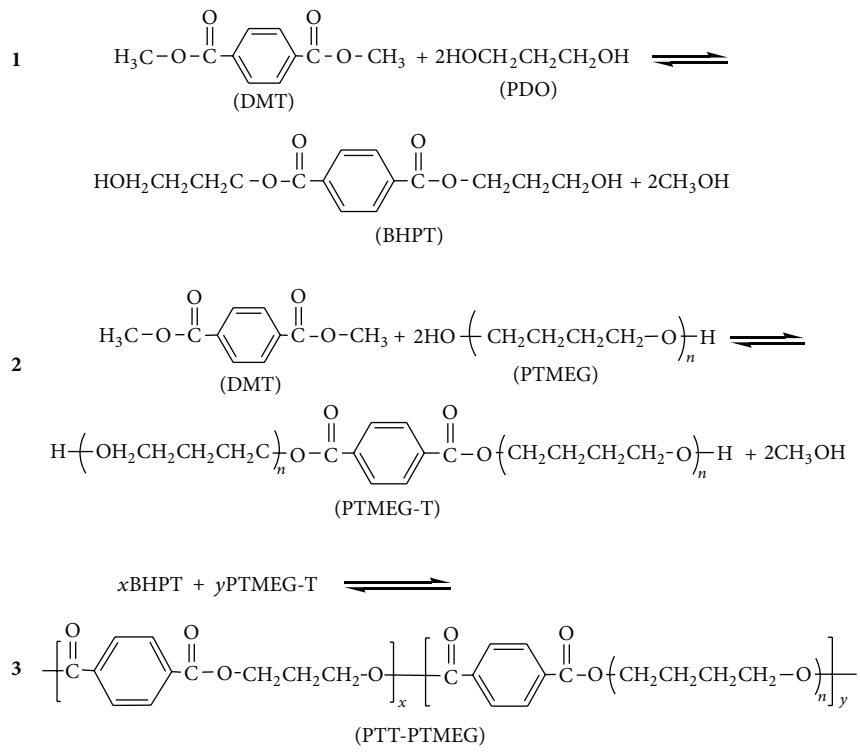

Scheme 1: Synthetic reactions of PTT-PTMEG.

been strong competitive power due to its excellent properties including good tensile behavior, resilience, outstanding elastic recovery, and dyeability, which make it an ideal candidate for use in applications such as textile fibers, carpets, or as an engineering plastic [11–13]. PTT has been received much attention from many industrial and academic research institutions [14–18]. As we know, less research work on TPEE based on PTT as rigid segments has been reported [19, 20]. In the US Patent [19], a PTT-based polyether-ester elastomer was synthesized comprising polytrimethylene ether-ester flexible segment and tetramethylene ester rigid segment. Szymczyk et al. [20] synthesized multiblock poly(ether-ester)s based on PTT as rigid segments and studied the PTT contents on the properties of the copolymers; the results suggest that a copolymer composed of 50% rigid segments has preferred properties.

In this work, a series of poly(trimethylene terephthalate)-*b*-poly(tetramethylene glycol) (PTT-PTMEG) copolymers were synthesized, and their chemical structure, crystal morphology, thermostability, crystallization and melting behaviors, mechanical properties, and rheology were studied in detail. Additionally, a PTT-PTMEG composed of the same mole ratio of rigid segments to soft segments (PTT : PTMEG = 75 mol% : 25 mol%) was synthesized and compared with the properties of a commercial PBT-type TPEE (PBT : PTMEG = 75 mol% : 25 mol%). The PTT-PTMEG copolymers are expected to possess good thermoplastic elastomer properties, such as low glass transition temperature (T_g), a relatively high melting point (T_m), and a temperature independent rubbery plateau.

2. Experimental

2.1. Materials. Dimethyl terephthalate (DMT), AR, Sinapharm Chemical Reagent Co., LTD, China; 1,3-propanenediol (PDO), AR, Tianjin Guangfu Fine Chemical Industry Research Institute, China; poly(tetramethylene glycol) with the molecular weight of 1000 g/mol (PTMEG), AR, Du Pont Co., USA; PBT-type TPEE (PBT% = 75 mol%, PTMEG% = 25 mol%), CH765, Sichuan Sunshine Plastic CO., Ltd.; and as the catalysts, tetrabutyl titanate ($Ti(OBu)_4$, Tianjin Kermel Chemical Reagent Co., Ltd.) and the antimony trioxide (Sb_2O_3, Tianjin Chemical Reagent Factory) were used. As the solvents, the phenol (Tianjin Kermel Chemical Reagent Co., Ltd) and the tetrachloroethane (Tianjin Guangfu Fine Chemical Industry Research Institute, China) were used. As an antioxidant, the tetrakis(methylene(3,5-di-t-butyl-4-hydroxyphenylhydro-cinnamate))methane (1010, Beijing Dilong Chemical Co. Ltd, China) was used.

2.2. Synthesis of PTT-PTMEG. The synthesis of poly(trimethylene terephthalate)-*b*-poly(tetramethylene glycol) (PTT-PTMEG) copolymers was shown in Scheme 1. These copolymers were prepared by conventional melt transesterification and polycondensation methods, and the products are linear multiblock copolymers with random distribution of the rigid and flexible segments. The reaction was carried in a vacuum flask equipped with a condenser, a stirrer, and a nitrogen atmosphere inlet. The reactions were described as follows: a mixture of DMT, PDO, PTMEG, $Ti(OBu)_4$ (DMT : $Ti(OBu)_4$ = $1 : 2 \times 10^{-4}$(mol : mol)), and 1010 (0.5% of total comonomers mass) was put into the flask under N_2

atmosphere. The mixture was heated to 220°C at a heating rate of 20°C/min and held at 220°C for 1.5 h, then Sb_2O_3 ($DMT : Sb_2O_3 = 1 : 2 \times 10^{-3}$ (mol : mol)) was added into the flask and the mixture was slowly heated to 230°C and kept for 0.5 h to reach the endpoint of transesterification, then the melt was heated and kept at 255–265°C under gradually reduced pressure (the final pressure was 60–70 Pa) for a period of time to acquire satisfied molecular weight. Finally, the resulting copolymer was extruded from flask under nitrogen, cooled to room temperature by water, and granulated, dried in a vacuum oven.

2.3. FTIR Analysis. FTIR spectra were recorded with a Varian-640 spectrophotometer (KBr pellet technique) in the wavenumbers from 4000 to 500 cm^{-1} with a resolution of 1 cm^{-1} and averaged over 48 scans.

2.4. Nuclear Magnetic Resonance (^1H NMR) Analysis. The ^1H NMR spectra were recorded by an AVIII type NMR 600 MHz spectrometer (Bruker BioSpin Co., Germany). CF_3COOD was used as a solvent.

2.5. Intrinsic Viscosity Characterization. The intrinsic viscosity of PTT-PTMEG copolymers was measured at 25 ± 0.1°C on an Ubbelohde viscometer (DC9V/0, Schott Co., Germany) using a mixed solvent of phenol/tetrachloroethane (50 wt/50 wt). Because the Mark-Houwink constant is not known for PTT-PTMEG copolymers, the Mark-Houwink relationship determined for PTT $[\eta] = 2.11 \times 10^{-5} M_w^{0.98}$ [21] was used to calculate the molecular weight of PTT-PTMEG. The intrinsic viscosity and the molecular weight of the various samples were listed in Table 1.

2.6. Differential Scanning Calorimetry Characterization. The melting and crystallization measurements were performed on a Perkin-Elmer Diamond DSC instrument (USA), which was calibrated with indium; the weights of the samples were approximately 6.0 mg. The dried samples were heated to 260°C from −30°C at a rate of 10°C/min under nitrogen atmosphere, held for 5 min, then cooled to 30°C at a rate of 10°C/min, held for 5 min, and finally heated again to 260°C at a rate of 10°C/min; the first and the second melting and the first cooling processes were recorded, respectively.

The samples were also heated to 260°C from 30°C at a rate of 80°C/min under nitrogen atmosphere, held for 5 min, and then quickly quenched to −50°C under a cooling rate of 100°C/min (the fastest cooling rate of the DSC used), then held at −50°C for 5 min. Subsequently, the glass transition temperature (T_g), cold-crystallization temperature (T_{cc}), and melting point temperature (T_m) were measured by heating the sample to 260°C at a heating rate of 10°C/min.

2.7. Polarized Optical Microscopy Characterization. The spherulites morphology was observed on a polarized optical microscopy (BX-51, Olympus, Japan) with a digital camera system. Samples were pressed between two glass slides with a separating of 100 μm after first melting on a hot stage at 250°C for 5 min; they were then cooled to room temperature at a cooling rate of 1°C/min, with the photographs taken at room temperature.

Table 1: Intrinsic viscosity and molecular weight of the various samples.

PTT/PTMEG (wt%/wt%)	$[\eta]$ (dL/g)	M_w (g/mol)
C0-100/0	0.3027	17400
C1-83/17	0.4481	26000
C2-66/34	0.2763	15900
C3-40/60	0.4827	28080

2.8. Thermostability Characterization. The thermostability testing was performed on a Perkin-Elmer Pyris 6 type TG instrument (USA), and the samples' weight was about 6.0 mg. The dried samples were heated from 30°C to 700°C at a rate of 20°C/min under nitrogen atmosphere; the weight loss behaviors were recorded.

2.9. Rheological Characterization. The copolymer sheets were made into standard wafers with size of $\phi 25 \times 2$ mm using a micro-injection molding machine (SZ-15, Wuhan Ruiming Machinery, China) with cylinder temperature in the range of 200–250°C and a mold temperature of 20°C. The dynamic rheological property of the copolymers was performed on a rotational rheometer (AR2000ex, Waters-TA Co., USA) with the plate diameter of 25 mm and a gap width of 1.0 mm. The frequency scan was from 0.628 to 628 rad/s and the testing temperature was held on 240°C with N_2 protection.

2.10. Mechanical Properties Testing. The tensile testing was done according to the ASTMD 638-99 normative with 1BA type specimens on a universal testing machine (WSM20, Changchun Intelligent Instrument & Equipment Co. Ltd, China) at room temperature, using the crosshead speed of 10 mm/min. Charpy impact tests were carried out according to the ISO 179-1982 standard using samples with V-notch splines and an impact tester (JJ-20, Changchun Intelligent Instrument Co. Ltd., China); the data reported were the mean and standard deviation from five determinations. Hardness measurements were performed on a Shore D apparatus (HT-6510D, Landtek Apparatus Co., China) according to a standard DIN 53505 and ISO 868.

3. Results and Discussions

3.1. Chemical Structure of PTT-PTMEG Copolymers. The FTIR spectra of PTT-PTMEG copolymer is shown in Figure 1. The vibration at 1712 cm^{-1} corresponds to C=O stretching vibration of the terephthalate units. Those vibrations at 1265 and 1132 cm^{-1} correspond, respectively, to C–O–C asymmetric and symmetric stretching vibration. The vibration at 726 cm^{-1} corresponds to $-CH_2-$ rocking vibration of the PTMEG units and those vibrations at 2951 cm^{-1} and 2856 cm^{-1} correspond, respectively, to $-CH_2-$ asymmetric and symmetric stretching vibration. The vibrations at 1503 and 1463 cm^{-1} correspond to C=C stretching vibration of

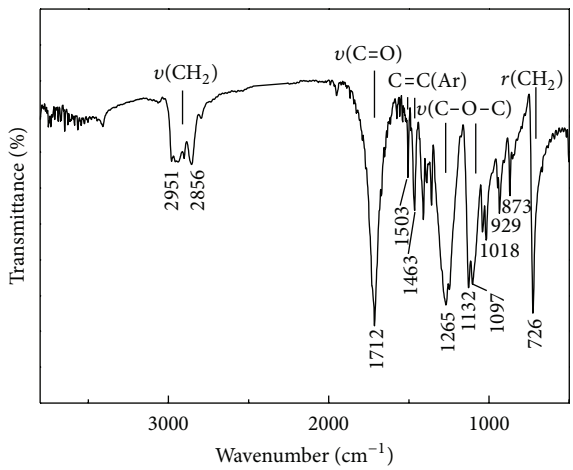

Figure 1: FTIR spectra of PTT-PTMG copolymer.

the phenyl group, and those vibrations at 1018 and 829 cm^{-1} correspond, respectively, to the C–H out-plane and in-plane deformation vibration of paradisplacement benzene ring.

The ^{1}H NMR spectra of PTT-PTMEG copolymers is shown in Figure 2. In ^{1}H NMR spectra, the chemical shifts at 2.58 ppm (peak a; 2H, C–CH_2–C) and at 4.84 ppm (peak b; 4H, O–CH_2–C) were mainly the methylene protons of the short chain diol (PDO). The signals at 8.31 ppm (peak c; 4H) correspond to the aromatic proton of the terephthalate units. The chemical shifts at 3.74 ppm (peak e; O–CH_2–C) and at 1.7 ppm (peak f; C–CH_2–C) were for the methylene protons of the PTMEG repeating blocks. Small signals at 4.55 ppm (peak h; COO–CH_2–C) correspond to the methylene protons neighboring to the ester group in the chain of PTMEG. The signals at 11.5 ppm correspond to the proton of TFA as a solvent.

PTT-PTMEG copolymer can be presented as linear multiblock copolyester composed of rigid and soft units. It gives possibility to calculate the degree of polymerization of the rigid segment, and the rigid segment content has been calculated based on the conventional soft segments definition, which includes one terephthalate unit (T) with each PTMEG sequence and called PTMEG-T as illustrated in Scheme 1. In Scheme 1, x is the degree of polymerization of the rigid segment (where $y = 1$, $n = 13.6$). The weight and mole fraction of rigid and flexible segments were calculated from the ^{1}H NMR spectra according to (1)–(3) and are listed in Table 2. The average length of the rigid PTT segments was also calculated from the ratio ($b : h$ in Figure 2) of the peak intensities, based on the assumption that flexible segment length is equal to the length of starting PTMEG. The calculated degree of polymerization of the PTT segments (x) in the macrochain from ^{1}H NMR spectra was between 24.1 (C1) and 2.3 (C3). For all the samples with exception of C1, the difference between the experimental (Exp) and theoretical (Theo) composition was less than 2%. Consider

$$x = \frac{b}{h}, \tag{1}$$

$$n = \frac{e}{h}, \tag{2}$$

$$\text{PTT (mol\%)} = \frac{x}{(1+x)}. \tag{3}$$

The results from FTIR and ^{1}H NMR measurements for the PTT-PTMEG copolymers suggest that the products are basically consistent with our expected chemical structures, as shown in Figure 2.

3.2. Melting and Crystallization Behaviors. Figure 3 shows the glass transition temperatures of the various copolymers, and the parameters are listed in Table 3. It can be seen in Figure 3 that C0 (pure PTT) and C1 only show one glass transition (T_{g1}) and a cold-crystallization peak (T_{cc}) in each DSC curve, in which T_{g1} and T_{cc} of C1 are much lower than those of C0, while, for C2 and C3, they both show two glass transitions (T_{g1} and T_{g2}) but without any cold-crystallization behavior. In Table 3, C0 has the largest value of T_{g1} among these samples, while T_{g1}s of C1, C2, and C3 decrease slightly; additionally, C3 has a larger T_{g2} than that of C2. There may be a mixed amorphous phase of PTT and PTMEG (T_{g1}s of C2 and C3 that are lower than that of C0) and an amorphous PTMEG phase (T_{g2}) occurred in the materials, so they both show two glass transitions in C2 and C3 copolymers.

Figure 4 shows the DSC melting thermograms of the various samples with the crystallization parameters summarized in Table 3. It can be seen from Figure 4 and Table 4 that these DSC curves have one or two asymmetrical melting peaks (T_{m1}, T_{m2}), and they tend to be narrow and shift to higher temperature with increasing PTT content in the copolymers because more PTT content will improve the regularity of molecular chains and the crystallizability of the copolymer; that is to say, when the PTT content increases, the longer rigid and crystallizable chain segments will form in the copolymers, so the longer and rigid segments will crystallize into larger crystals and they will melt at higher temperature. The multiple melting peaks behavior may be due to the different kinds of the copolymers formed with different length of rigid segments. The melting enthalpy (ΔH_m) also decreases greatly with increasing PTEMG content in the copolymers.

In addition, except for the sample C3, each of the curves exhibits a recrystallization peak (T_{re}) before the melting peak, which shifts to higher temperature with increasing PTT rigid segments content. This result is also correlated to the molecular structure of the copolymer. Because the sample with more PTMEG content has lower crystallizability, some microcrystallites with lower perfection and smaller size will form in the material; these microcrystallites will melt and recrystallize at low temperatures in the heating process. The sample C3 having the most PTMEG contents in the copolymer shows no recrystallization peak because of its lowest crystallizability. The recrystallization enthalpy (ΔH_{re}) also decreases with increasing PTMEG content in the copolymers. On the other hand, in the DSC curves of C2 and C3, the melting peaks are shown with much wide distribution, indicating that the length of the rigid segments may have a wide distribution in the copolymers and they form spherulites with different sizes that melt at different temperatures.

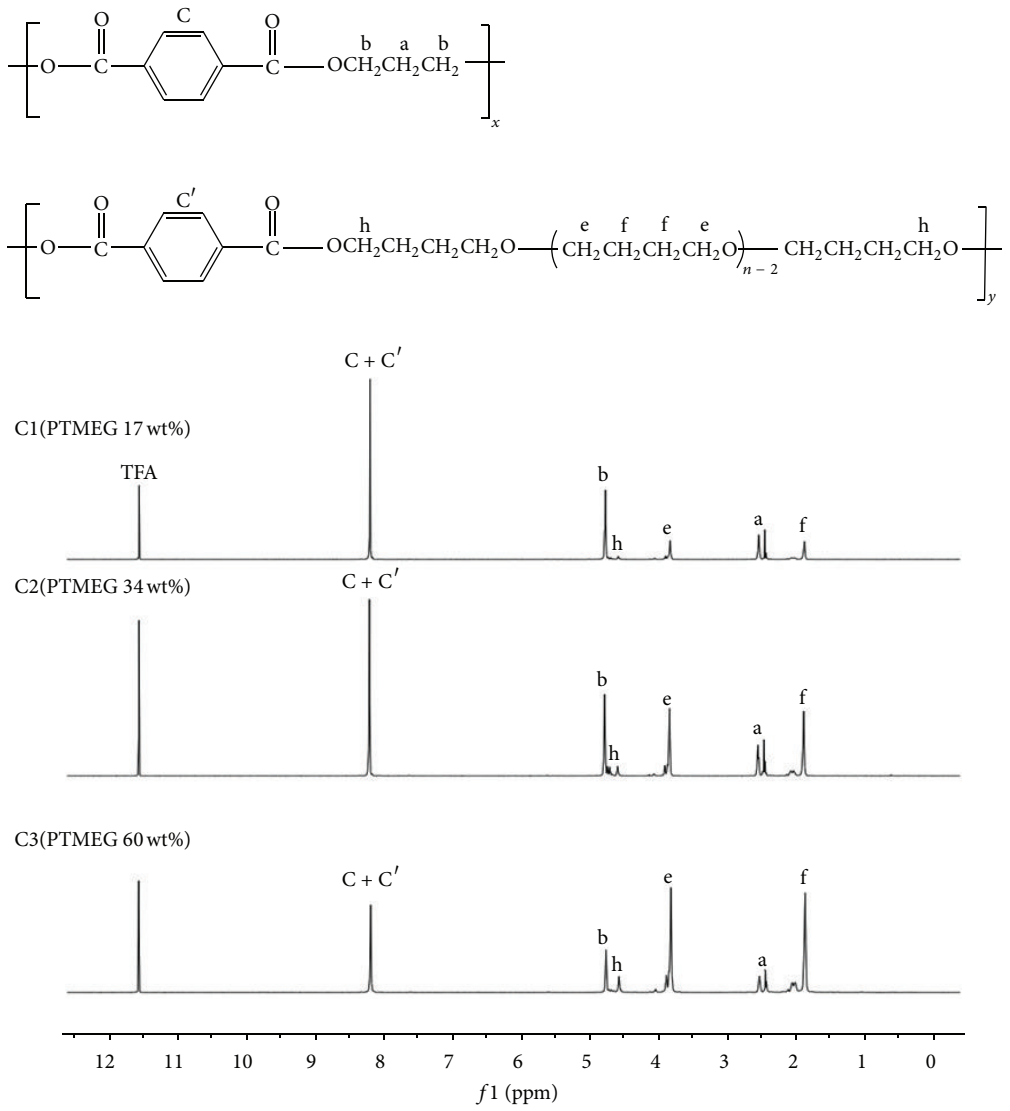

Figure 2: ^{1}H NMR spectra of PTT-PTMEG copolymers.

Table 2: The composition of the synthesized PTT-PTMEG copolymers determined from ^{1}H NMR spectra.

PTT/PTMEG (wt%/wt%)	PTT (mol%)		PTT (wt%)		x		PTMEG (mol%)		PTMEG (wt%)		n	
	Theo	Exp	Theo	Exp	Theo	Exp	Theo	Exp	Theo	Exp	Theo	Exp
C1-83/17	96.0	94.8	81.5	76.9	24.1	18.2	4.0	5.2	18.5	23.1	13.6	11.2
C2-66/34	90.0	89.2	62.1	60.1	9.0	8.3	10.0	10.8	37.9	39.9	13.6	12.6
C3-40/60	70.0	71.4	29.8	31.3	2.3	2.4	30.0	28.6	70.2	68.7	13.6	11.9

Table 3: DSC melting and crystallization parameters of the various samples.

PTT/PTMEG (wt%/wt%)	First heating process								Cooling process		
	T_{g1} (°C)	T_{g2} (°C)	T_{cc} (°C)	T_{re} (°C)	ΔH_{re} (J·g^{-1})	T_{m1} (°C)	T_{m2} (°C)	ΔH_m (J·g^{-1})	T_c (°C)	ΔH_c (J·g^{-1})	FWHP (°C)
C0-100/0	—	49.3	67.8	199.3	−7.05	—	229.2	62.01	202.8	−57.88	8.6
C1-83/17	—	26.4	49.7	188.3	−5.37	208.6	221.8	48.96	191.4	−41.69	8.7
C2-66/34	−64.5	24.7	—	166.7	−3.48	199.8	206.7	42.41	185.3	−40.83	12.7
C3-40/60	−67.7	22.5	—	—	—	—	180.7	25.19	160.8	−15.81	13.9

Table 4: Parameters of the TGA curves for the various samples.

PTT/PTMEG (wt%/wt%)	$T_{2\%}$ (°C)	$T_{5\%}$ (°C)	T_{max} (°C)	$W_{600°C}$ (%)	η_0* (Pa·s)	σ_t[a] (MPa)	ε_b[b] (%)	σ_i[c] (KJ·m^{-2})	H[d] (Sh D)
C0-100/0	343.8	369.0	406.5	0.69	345.1	30.4	33.3	7.6	76
C1-83/17	345.8	367.9	409.9	0.75	230.2	11.4	249.1	16.5	58
C2-66/34	324.3	362.4	408.0	0.83	168.8	8.7	398.6	28.8	41
C3-40/60	274.8	351.3	408.0	0.26	111.5	5.8	589.1	47.2	26

[a]Tensile strength.
[b]Elongation at breaking point.
[c]Impact strength.
[d]Shore hardness.

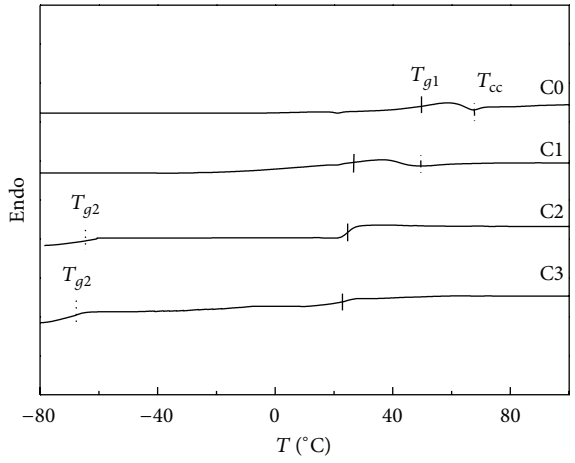

Figure 3: Glass transitions of the various copolymers.

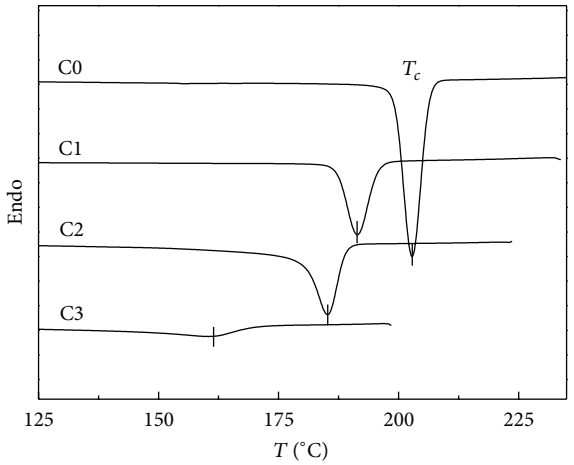

Figure 5: DSC crystallization curves of the various samples.

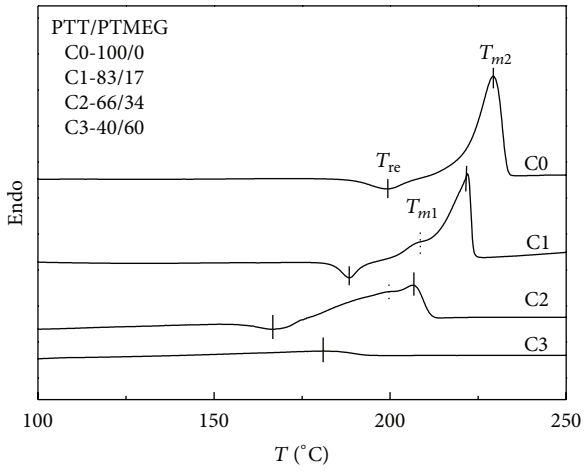

Figure 4: DSC first melting thermograms of the various samples.

Figure 5 shows the DSC melt-crystallization curves of the various samples and their crystallization parameters were summarized in Table 3. As seen from Figure 5, except for C3, each of the curves is shown with good symmetrical crystallization peak, and they also tend to be narrow and shift to high temperature with increasing PTT contents. The crystallization enthalpy (ΔH_c) also increases with increasing PTT contents. Moreover, the full width at half-height of the crystallization peak (FWHP) decreases as PTT content increases. It can be concluded that the sample with higher PTT content has higher onset-crystallization temperature and faster crystallization rate. Their crystallization behaviors are also correlated to the content of the rigid segments, as explained above. The sample C3 has an unobvious crystallization peak mainly because of its lower crystalline content of rigid PTT.

From the above results of glass transitions, cold-crystallization, melting points, and crystallization behaviors of the various copolymers, we may give the following conclusions: (1) there may be four different domains in the copolymers: a crystalline PTT phase, an amorphous PTT phase, an amorphous PTMEG phase, and a mixed amorphous phase depending on the sample composition. When PTMEG content is 17 wt% (C1), a mixed amorphous phase shows lower T_{g2} and T_{cc} than those of C0; when PTMEG contents are 34 wt% (C2) and 60 wt% (C3), both a mixed amorphous phase and an amorphous PTMEG phase occur in the materials, so they both show two glass transitions (T_{g2} and T_{g1}). The presence of four different domains depends on the thermal history and composition in the elastomers based on PET and PEO which have been observed by Fakirov et al. [22]. (2) When the PTT-PTMEG copolymers contain above 34 wt% of soft segments, low-temperature glass transition and a high

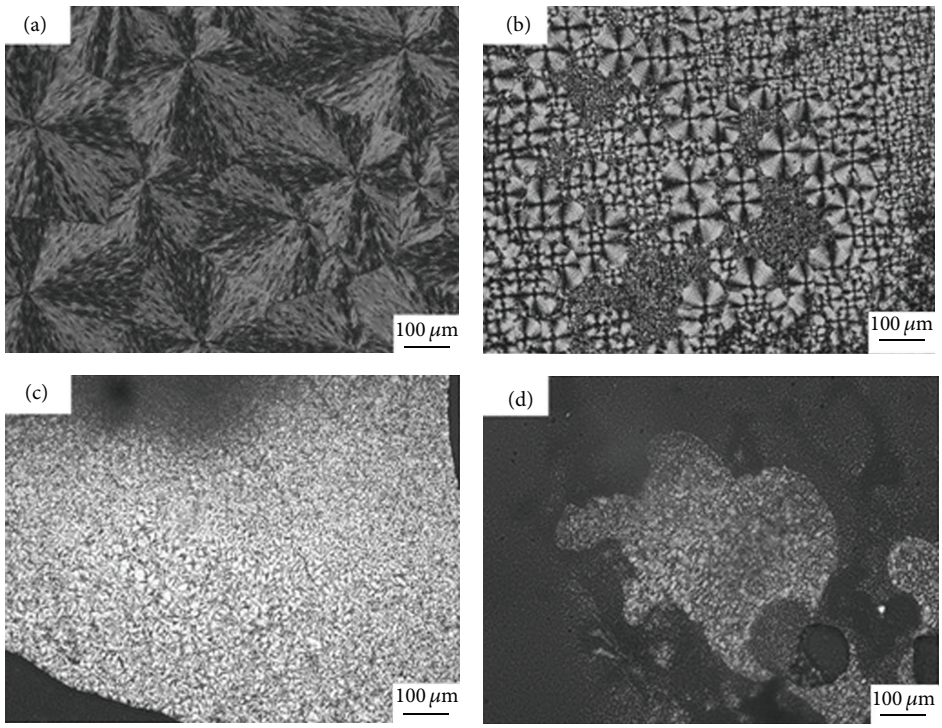

Figure 6: POM micrographs of crystallized samples (a) C0; (b) C1; (c) C2; and (d) C3.

melting point can be observed, thus the microphase separation structure occurred in the copolymers, which are two important characters for the thermoplastic elastomers.

3.3. Spherulite Morphology. Figure 6 shows the spherulite morphology of the various samples. As seen in Figure 6(a), the spherulites of PTT are fairly large with perfect Maltese cross extinctions, while for C1 (Figure 6(b)), it exhibits a relatively well-defined spherulitic texture with Maltese cross extinctions but with small spherulite size; additionally, some microspherulites are observed in some area. As shown in Figures 6(c) and 6(d), C2 and C3 images exhibit large number of small bright spots, and nearly no clear Maltese cross extinctions can be observed, indicating that only some microcrystallites can be formed in these samples. The above results suggest that the spherulite size of PTT-PTMEG copolymers decreases with the decreasing contents of rigid PTT segments. We believe that the crystallization behavior of PTT segments is limited by the soft PTMEG segments, and PTMEG and some uncrystallized PTT form the amorphous phase in the material.

3.4. Thermal Stability. Figure 7 shows the TG curves of the various samples and the parameters are listed in Table 4. It can be seen that each curve has one predominant degradation stage. The temperatures at weight losses of 2% ($T_{2\%}$) and 5% ($T_{5\%}$) decrease with increasing soft PTMEG segments, while the fastest thermolysis temperatures (T_{max}) and the residues weight ($W_{600^\circ C}$) are nearly the same at 600°C. These results suggest that the thermal stability of the copolymers becomes worse with more soft PTMEG content.

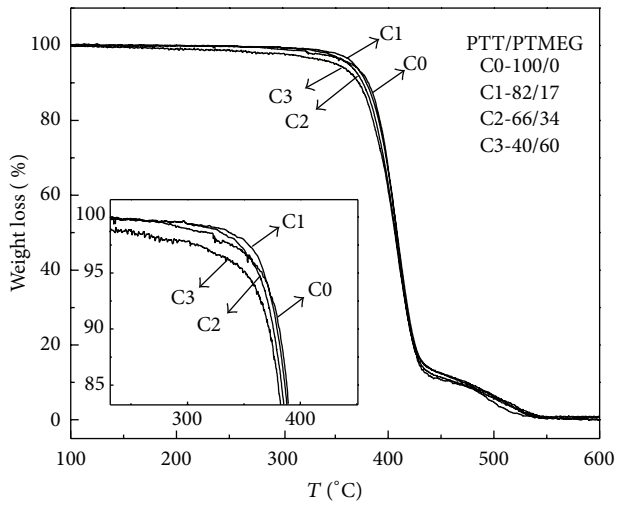

Figure 7: TG curves of the various samples.

3.5. Rheology Behaviors. Figure 8 is the plots of complex viscosity versus frequency (η^*-ω) of different samples. For PTT, its complex viscosity remains nearly stable as $\omega < 10^2$ rad/s, indicating that PTT melt is Newtonian liquid at low shearing frequencies, while it turns into pseudoplastic fluid as $\omega < 10^2$ rad/s. In the low shearing frequencies range, the entangling rate and unentangling rate of molecular chains achieve a dynamic balance, so the complex viscosity presents a platform. When the shearing frequency exceeds a critical value, the unentangling rate is faster than entangling rate, so

Table 5: DSC melting and crystallization parameters of the various samples.

Sample	$[\eta]$ (dL/g)	M_w (g/mol)	T_g (°C)	T_m (°C)	ΔH_m (J·g^{-1})	T_c (°C)	ΔH_c (J·g^{-1})	FWHP (°C)
PBT-type	0.50	28919	12.6	204.7	29.38	155.2	−35.06	21.2
PTT-type	1.02	60274	−68.1	171.9	31.36	101.6	−21.93	25.7

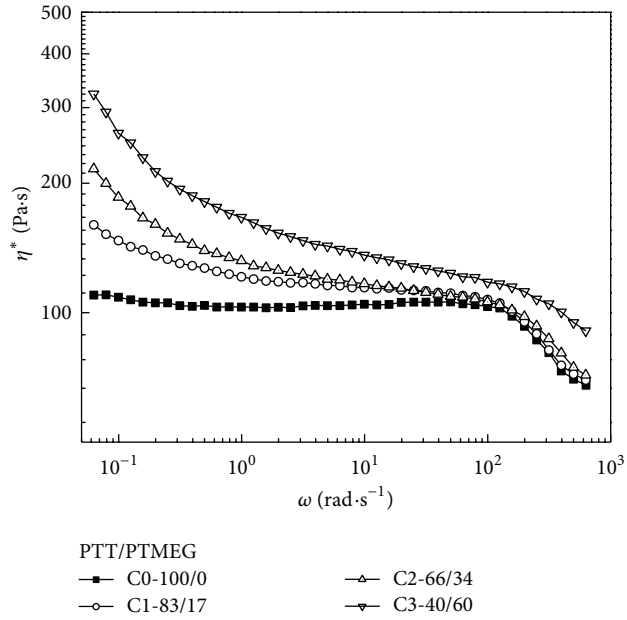

Figure 8: Curves of η^* versus ω of the various copolymers.

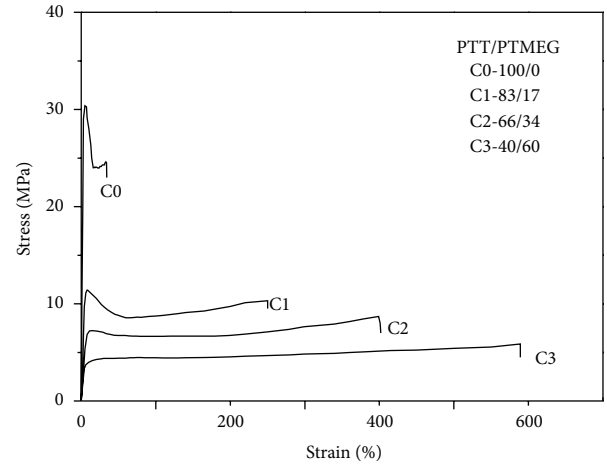

Figure 9: The stress-strain properties of PTT-PTMEG copolymers.

the complex viscosity decreases. On the other hand, it can be seen from Figure 8 that the copolymer with more PTMEG content has larger zero shear viscosity (η_0^*) values (Table 4), suggesting that the copolymer with more flexible segments can form more entangled points in the polymer. For three copolymers, their η^* slowly decreases first, then remains stable and then decreases at high shearing frequency. Because PTT-PTMEG copolymers have more flexible segments than that in pure PTT, there are more entangled points in the copolymers, and some entangled points are easily destroyed at low shearing frequency, so the η^* decreases at low frequencies range and the more the flexible PTMEG contents in the copolymers, the more sharply the decrease of η^*. The three copolymers are pseudoplastic fluids at low shearing frequencies. At high frequencies, their η^* values are close to each other due to the high shearing rate which makes most entangled points unentangle.

3.6. Mechanical Properties. The mechanical properties of the various copolymers are tested and their stress-strain curves are shown in Figure 9 and the data are listed in Table 4. It can be seen that the tensile strength decreases while the elongation at breaking point increases with increasing flexible segments (Table 4). These results are mainly because of the decrease of the crystallinity in the copolymers. On the other hand, as shown in Table 4, the impact strength increases and the Shore hardness decreases with increasing soft PTMEG segments in the copolymers.

3.7. Comparison of PTT-Type TPEE and PBT-Type TPEE. In this part, in order to compare the properties of the copolymer based on PTT as rigid segments (PTT-type TPEE) to the commercially produced TPEE based on PBT as rigid segments (PBT-type TPEE), a PTT-type TPEE copolymer composed of PTT rigid segments of 75 mol% was synthesized; that is, it has the same compositions of commercially produced PBT-type TPEE (PBT mol% = 75%), and their thermal and mechanical properties were characterized. In Table 5, PTT-type TPEE has higher (η) and M_w than those of PBT-type TPEE. Figure 10 shows the DSC melting thermograms of the PTT-type TPEE and PBT-type TPEE samples, and the crystallization parameters are summarized in Table 5. It can be seen that PBT-type TPEE's DSC curve has higher glass transition temperature (T_g) and melting point (T_m) than those of PTT-type TPEE. Figure 11 shows the DSC crystallization curves of PTT-type TPEE and PBT-type TPEE samples with the crystallization parameters summarized in Table 5. It can be seen that PBT-type TPEE's crystallization peak value (T_c), and crystallization enthalpy (ΔH_c) are both larger than those of PTT-type TPEE, while its FWHP is lower than that of PTT-type TPEE. These results suggest that PBT-type TPEE has higher crystallization temperature and larger crystallization rate and material crystallinity than those of PTT-type TPEE.

Figure 12 shows the TG curves of PTT-type and PBT-type TPEE samples and the parameters are listed in Table 6. It can be seen that PTT-type TPEE has a better thermostability than that of PBT-type TPEE.

The mechanical properties of PTT-type and PBT-type TPEEs' tensile curves are shown in Figure 13, and the data are also listed in Table 6. It can be seen that PTT-type TPEE's stress-strain curve is a typical elastic curve with large elongation at breaking point but without yield behavior, while, for

Table 6: TG parameters and mechanical properties for PBT-type and PTT-type TPEE.

TPEE	$T_{5\%}$ (°C)	T_{max} (°C)	σ_t (MPa)	E^a (MPa)	ε_b (%)	σ_i (KJ·m^{-2})	H (Sh D)
PBT-type	385.8	428.3	26.0	322	291	9.6	39
PTT-type	370.3	425.7	4.4	24.8	647	51.3	22

[a]Elastic modulus.

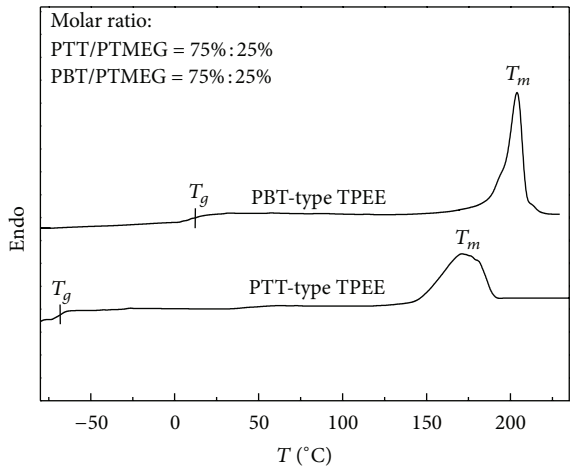

Figure 10: DSC melting curves of two copolymers.

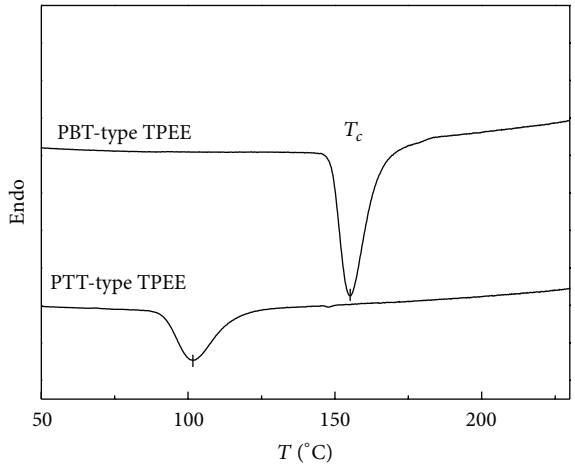

Figure 11: DSC crystallization curves of two copolymers.

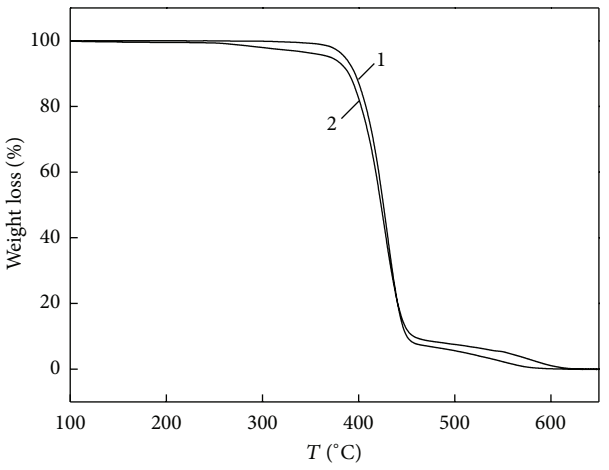

(1) PBT-type TPEE
(2) PTT-type TPEE

Figure 12: TG curves of two copolymers.

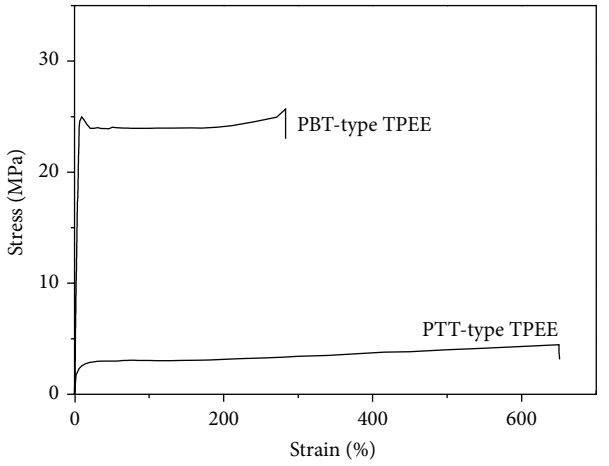

Figure 13: The stress-strain curves of two copolymers.

that of PBT-type TPEE, it shows a small yield behavior with lower elongation at breaking point. PBT-type TPEE has much larger tensile strength and modulus than those of PTT-type TPEE.

Moreover, PTT-type TPEE has much larger impact strength than those of PBT-type TPEE (Table 6), and the hardness of PTT-type TPEE is smaller than that of PBT-type TPEE due to its larger crystallinity.

As we know, PBT molecular chains are more flexible than that of PTT, and PBT segments can crystallize at fast crystallization rate at high temperature; therefore, PBT-type TPEE has higher melting point than that of PTT-type TPEE. PBT-type TPEE's high tensile strength and hardness are also due to its larger crystallinity, while PTT-type TPEE's larger impact strength is due to its lower crystallinity and lower glass transition temperature. However, although this PTT-type TPEE has large impact stress, it is not suitable to be used as a commercial TPEE with this mole ratio of rigid and soft segments because of its low tensile strength. PTT-type TPEE containing less than 25 mol% PTMEG may be more suitably served as thermoplastic elastomer because of its high melting point, fast crystallization rate, and a relatively lower glass transition temperature.

4. Conclusions

A series of poly(trimethylene terephthalate)-*b*-poly(tetramethylene glycol) (PTT-PTMEG) copolymers can be synthesized by conventional two-step melt polycondensation. By increasing the flexible segment contents, the copolymers show lower glass transition temperatures, melting points, melt-crystallization temperature, less thermostability, lower tensile strength, and smaller spherulites size; however, the complex viscosity, the elongation at breaking point, and impact strength increase with increasing flexible segments. Compared with PBT-type TPEE, PTT-type TPEE has lower glass transition temperatures, melting and crystallization temperature, crystallinity, lower tensile strength, and lower hardness but higher impact stress. PTT-type TPEE containing less than 25 mol% PTMEG may be more suitably served as thermoplastic elastomer.

Acknowledgment

The authors are grateful for the support by the Natural Science Foundation of Hebei Province (Contract Grant no.: B2010000219).

References

[1] Z. Roslaniec, "Polyester thermoplastic elastomers: synthesis, properties, and some applications," in *Handbook of Condensation Elastomers*, S. Fakirov, Ed., chapter 3, pp. 77–116, Wiley-VCH, Weinheim, Germany, 2005.

[2] R. K. Adams, G. K. Hoeschele, and W. K. Witsiepe, "Thermoplastic polyether-ester elastomers," in *ThermoPlastic Elastomers*, G. Holden, H. R. Kricheldorf, and R. P. Quirk, Eds., chapter 8, pp. 183–216, Hanser, Munich, Germany, 2004.

[3] G. Holden, N. R. Legge, H. E. Schweder, and R. P. Quirk, *Thermoplastic Elastomers*, Chemical Industry Press, Beijing, China, 2000.

[4] J. J. Zeilstra, "Influencing the crystallization behavior of pet-based segmented copoly(ether ester)," *Journal of Applied Polymer Science*, vol. 31, no. 7, pp. 1977–1997, 1986.

[5] Z. Roslaniec and D. Pietkiewicz, "Synthesis and characteristics of polyester-based thermoplastic elastomers: chemical aspects," in *Handbook of Thermoplastic Polyesters: Homopolymers, Copolymers, Blends, and Composites*, S. Fakirov, Ed., chapter 13, pp. 581–642, Wiley-VCH, Weinheim, Germany, 2002.

[6] Y. Nagai, D. Nakamura, T. Miyake et al., "Photodegradation mechanisms in poly(2,6-butylenenaphthalate-co-tetramethyleneglycol) (PBN-PTMG). I: influence of the PTMG content," *Polymer Degradation and Stability*, vol. 88, no. 2, pp. 251–255, 2005.

[7] J. C. Stevenson and S. L. Cooper, "Multiple endothermic melting behavior in poly(tetramethylene terephthalate)-containing polyesters and block copolyetehr-esters," *Journal of Polymer Science, Part B*, vol. 26, no. 5, pp. 953–966, 1988.

[8] K. P. Perry, W. J. Jackson, and R. J. Caldwell, "Elastomers based on polycyclic bisphenol polycarbonates," *Journal of Applied Polymer Science*, vol. 9, no. 10, pp. 3451–3463, 1965.

[9] J. R. Whinfield and J. T. Dickson, "Improvements relating to the manufacture of highly polymeric substances," Br. Patent 578,079, 1941.

[10] J. R. Whinfield and J. T. Dickson, "Polymeric linear terephthalic esters," US 2465319 A, 1949.

[11] H. H. Chuah, "Orientation and structure development in poly(trimethylene terephthalate) tensile drawing," *Macromolecules*, vol. 34, no. 20, pp. 6985–6993, 2001.

[12] J. S. Grebowicz, H. Brown, H. Chuah et al., "Deformation of undrawn poly(trimethylene terephthalate) (PTT) fibers," *Polymer*, vol. 42, no. 16, pp. 7153–7160, 2001.

[13] J. Zhang, "Study of poly(trimethylene terephthalate) as an engineering thermoplastics material," *Journal of Applied Polymer Science*, vol. 91, no. 3, pp. 1657–1666, 2004.

[14] M. Run, Y. Wang, C. Yao, and H. Zhao, "Isothermal-crystallization kinetics and melting behavior of crystalline/crystalline blends of poly(trimethylene terephthalate) and poly(ethylene 2,6-naphthalate)," *Journal of Applied Polymer Science*, vol. 103, no. 5, pp. 3316–3325, 2007.

[15] W. Wang, M. Yao, H.-S. Wang, X. Li, and M.-T. Run, "Mechanical property, crystal morphology and nonisothermal crystallization kinetics of poly(trimethylene terephthalate)/maleinized acrylonitrile-butadiene-styrene blends," *Journal of Macromolecular Science, Part B*, vol. 52, no. 4, pp. 574–589, 2013.

[16] M. Run, Y. Hao, H. Song, and X. Hu, "Spherulite morphology and thermal behaviors of short carbon fiber/poly(trimethylene terephthalate) composites," *Journal of Macromolecular Science, Part B*, vol. 48, no. 1, pp. 13–24, 2009.

[17] J. Wang, C.-Z. Wang, H.-Z. Song, and M.-T. Run, "Dynamic rheological and dynamic thermomechanical properties of poly(trimethylene terephthalate)/short carbon fibre composites," *Composites Interface*, vol. 20, no. 5, pp. 355–363, 2013.

[18] J. Wang, C.-Z. Wang, and M.-T. Run, "Study on morphology, rheology and mechanical properties of poly(trimethylene terephthalate)/$CaCO_3$ nanocomposites," *International Journal of Polymer Science*, vol. 2013, Article ID 890749, 8 pages, 2013.

[19] E. I. du pont de nemours and company, "Polyether-ester elastomer comprising polytrimethylene ether-ester soft segment and tetramethylene ester hard segment," USA Patent 6562457, May 2003.

[20] A. Szymczyk, E. Senderek, J. Nastalczyk, and Z. Roslaniec, "New multiblock poly(ether-ester)s based on poly(trimethylene terephthalate) as rigid segments," *European Polymer Journal*, vol. 44, no. 2, pp. 436–443, 2008.

[21] A.-P. Li, W.-J. Han, and Y.-S. Chen, "Molecular weight measurement of poly(trimethylene terephthalate) using viscosity method," *Polyester Industry*, vol. 14, no. 2, pp. 19–22, 2001 (Chinese).

[22] S. Fakirov, A. A. Apostolov, P. Boeseke, and H. G. Zachmann, "Structure of segmented poly(ether ester)s as revealed by synchrotron radiation," *Journal of Macromolecular Science: Physics*, vol. B29, no. 4, pp. 379–395, 1990.